Proc. Natl. Acad. Sci. USA
Vol. 80, pp. 7234–7238, December 1983
Cell Biology

Steady-state theory of the interference of GTP hydrolysis in the mechanism of microtubule assembly

(GTP cap/discontinuity in assembly rate/stochastic analysis)

TERRELL L. HILL* AND MARIE-FRANCE CARLIER†

*Laboratory of Molecular Biology, National Institute of Arthritis, Diabetes, and Digestive and Kidney Diseases, National Institutes of Health, Bethesda, MD 20205; and †Laboratoire d'Enzymologie, Centre National de la Recherche Scientifique, 91190 Gif-sur-Yvette, France

Contributed by Terrell L. Hill, August 22, 1983

ABSTRACT **A model is presented for the interference of GTP hydrolysis in the mechanism of microtubule assembly. This model is suggested by previous results showing that both GTP and GDP are present at microtubule ends because of GTP hydrolysis and that tubulin does not bind to a GDP-bound end. The analytical theory developed here is aimed at calculation of the steady-state subunit flux at one end of the polymer. The GTP/GDP features just mentioned result in a nonlinear plot of the flux versus tubulin concentration. Microtubules are predicted to exhibit a different kinetic behavior below and above the critical concentration, which can be considered as a transition between two regimes.**

There is evidence (1) that GTP-tubulin (called T, below) forms a steady-state cap at and near an end of a microtubule, though in the deep interior the subunits of the polymer are all GDP-tubulin (called D, below). Until recently, it was thought that an added T hydrolyzes very quickly to D at the very tip of a microtubule so that the entire polymer would consist of, for practical purposes, D units only. In the newer view (1, 2), a given T unit that adds to the tip might be buried in the microtubule end but would eventually become D, if it did not first leave again. In steady-state growth (or even steady shortening), there would then be a certain statistical population of still-surviving T near the end of the microtubule—the GTP cap.

The steady-state kinetic theory of microtubule and actin polymerization (3, 4) therefore needs modification, at least for microtubules—and probably also for actin (5, 6). An attempt at this was made in ref. 4, where an "uncorrelated approximation" was used in the treatment of a single independent helix. In this paper, we give an exact analytical treatment of the problem that avoids the uncorrelated approximation but has to be limited to the special case (see Fig. 1) $\kappa = 0$, $\alpha_{1D} = 0$, except near $c = 0$ (c is the concentration of free T). Because the experimental values of κ and α_{1D} are both probably small, this treatment is probably fairly realistic. An interesting result is that the theory predicts a significant discontinuity in slope for the steady-state subunit flux as a function of c, at the critical concentration (where flux = 0).

THE MODEL

The explicit model we use here was introduced in appendix 3 of ref. 4, following Carlier (2). If we assume that a microtubule is, say, a five-start helix, then as an approximation we consider the five helices to be independent (4). As a consequence, the model and its rate constants relate to the kinetics of a single helix (a "polymer," below). We consider a single end only.

The types of transitions included in the model for, say, the α end of the polymer are shown in Fig. 1*a*, where T refers to a tubulin dimer (a "subunit") with GTP bound, D refers to a subunit with GDP bound, and the concentration of T in solution is c. All rate constants are first order except α_1, which is second order. T can attach to ($\alpha_1 c$) or detach from (α_{-1}) a polymer end (position $n = 1$ of the numbered subunits on a helix). These are the only reversible transitions in the model.

Actually, the on–off rate constants in Fig. 1*a* are not used as written there but rather are subdivided as shown in Fig. 1 *b* and *c*. The attachment (on) constant for a T from solution is α_{1T} onto a polymer T at $n = 1$ and is α_{1D} onto a polymer D at $n = 1$ (Fig. 1*b*). We generally assume that, according to experimental results (7), $\alpha_{1D} = 0$. The detachment (off) constants for T or D at $n = 1$ are assumed to depend on the state (T or D) of the neighbor at $n = 2$, as shown in Fig. 1*c*.

GTP hydrolysis accompanying polymerization is a single turnover reaction taking place on interior ($n \geq 2$) subunits of the polymer (1) with rate constant κ, which is relatively small. The resulting GDP is not exchangeable and the deep interior of the polymer is all D (8, 9). In contrast, at position $n = 1$, GTP can be hydrolyzed with rate constant κ', and subsequent exchange of GTP for GDP can take place with rate constant κ'' (2, 7). Consequently, the sequences $\alpha_{1T}c$, κ', α_{2T} or α_{2D} and κ', κ'' both complete a cycle of GTP hydrolysis at the polymer end. The reverse reactions of κ, κ', κ'', α_{2D}, and α_{2T} are neglected here. Exchange of GTP for GDP on a free subunit in solution is assumed to be fast.

In the analytical discussion given below, which is aimed primarily at the calculation of the subunit flux J_α, we take both $\alpha_{1D} = 0$ and $\kappa = 0$ at the outset. As a second-stage approximate correction, we can then introduce a small $\kappa > 0$. However, the relatively simple analysis that we are able to use here cannot be retained if $\alpha_{1D} > 0$. To treat $\kappa > 0$ and $\alpha_{1D} > 0$ exactly, Monte Carlo calculations are needed (10).

In view of the above comments, a few words about the special consequences of the condition $\alpha_{1D} = 0$ may be in order. In this case T from solution can attach only to an end T not to an end D (Fig. 1*b*). When c is very small ($c \ll c_\alpha$), the polymer loses subunits steadily ($J_\alpha < 0$). Hence, D subunits are being brought to the "surface" ($n = 1$) continually. Because T cannot attach to D ($\alpha_{1D} = 0$), the only way T can occur at the end ($n = 1$) is via the κ'' exchange reaction (when $c \to 0$). Thus, elongating sites capable of attaching T depend on the κ'' reaction at small c. If κ'' itself is relatively small, the increase of J_α with c will be very small. That is, there will be a long, almost flat, induction regime in the negative part of the $J_\alpha(c)$ curve at small c before significant T occurs at the polymer end and finally allows J_α to increase to $J_\alpha = 0$ at $c = c_\alpha$. At this point, a discontinuity in the slope of J_α occurs because of the fact that, since $\alpha_{1D} = 0$, α_{1T} dominates the slope of J_α when $J_\alpha > 0$ whereas a small κ'' dominates it when $J_\alpha < 0$. Because the negative branch of $J_\alpha(c)$ makes a much delayed increase toward $J_\alpha = 0$, $c = c_\alpha$,

The publication costs of this article were defrayed in part by page charge payment. This article must therefore be hereby marked "*advertisement*" in accordance with 18 U.S.C. §1734 solely to indicate this fact.

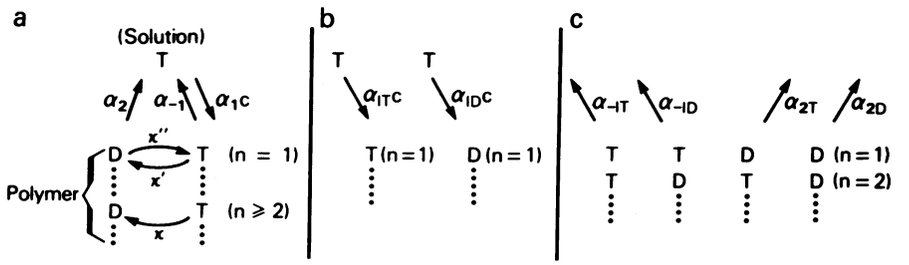

FIG. 1. (*a*) Classes of transitions and rate-constant notation included in the model considered in this paper. (*b*) Subdivision of "on" transitions, according to occupant of position $n = 1$. (*c*) Subdivision of the two kinds of "off" transitions, according to occupant of position $n = 2$.

when it does increase it must do so steeply. This steep slope is much larger than the modest slope in the $J_\alpha > 0$ branch.

The two regimes or branches are like two phases in a phase transition (strictly, a second-order phase transition). Of course the present system is a steady-state system not an equilibrium system. Qualitatively the primary reason why the two regimes are so different is that the lower regime is dominated by a steady stream of Ds moving to the polymer end or tip from the polymer interior whereas the upper regime is dominated by a steady stream of Ts coming to the polymer end from the surrounding solution. There is some resemblance here to a river mouth or estuary (the polymer end) that is influenced primarily by the river at low tide but by the ocean at high tide.

THEORY: UPPER BRANCH, $J_\alpha > 0$

As already mentioned, we start with $\alpha_{1D} = 0$, $\kappa = 0$ and modify later for a nonzero but small κ. In the growing branch of $J_\alpha(c)$—i.e., $J_\alpha > 0$—T from solution adds repeatedly to polymer T at $n = 1$, interspersed with departures of D or T from the $n = 1$ position. There is a long string of pure T starting with $n = 2, 3, \ldots$ (the GTP cap). With $\kappa = 0$, none of these can change to D, the cap never reaches a steady size, and there is no way for position $n = 2$ to be a D. Therefore, $p_2 = 1$. The string grows at a steady rate J_α, to be determined. The end of the polymer has only two states, shown in Fig. 2 with the transition rate constants. Adding or losing a T in state 1 still leaves the system in state 1. From Fig. 2, we have, at steady state:

$$p_1\kappa' = (1 - p_1)(\alpha_{2T} + \kappa'')$$

or

$$p_1 = \frac{\alpha_{2T} + \kappa''}{\alpha_{2T} + \kappa' + \kappa''}. \qquad [1]$$

This expression is independent of c. The net rate of adding subunits at c is then

$$J_\alpha = p_1\alpha_{1T}c - p_1\alpha_{-1T} - (1 - p_1)\alpha_{2T} = A + Bc, \qquad [2]$$

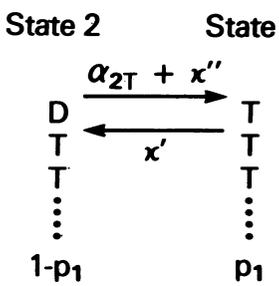

FIG. 2. The two states and transitions that need to be considered when $J_\alpha > 0$ and $\kappa = 0$, $\alpha_{1D} = 0$.

where

$$A = \frac{-(\alpha_{2T} + \kappa'')\alpha_{-1T} - \alpha_{2T}\kappa'}{\alpha_{2T} + \kappa' + \kappa''}$$
$$B = \frac{(\alpha_{2T} + \kappa'')\alpha_{1T}}{\alpha_{2T} + \kappa' + \kappa''}. \qquad [3]$$

Thus, J_α is a straight line with slope B and (hypothetical) intercept A. The value of the critical concentration c_α from this branch is found by putting $J_\alpha = 0$:

$$c_\alpha = -A/B = \frac{(\alpha_{2T} + \kappa'')\alpha_{-1T} + \alpha_{2T}\kappa'}{(\alpha_{2T} + \kappa'')\alpha_{1T}}. \qquad [4]$$

Of course Eq. 2 is strictly applicable only when $J_\alpha > 0$—that is, when $c > c_\alpha$. However, this same value of c_α is also found from the lower branch $J_\alpha < 0$ (see below).

The steady-state rate of hydrolysis of GTP is simply $J_h = \kappa' p_1$, a constant.

Introduction of $\kappa > 0$. When κ is small, but not zero, specifically $0 < \kappa \ll J_\alpha$, the values of the first few p_n after p_1 (i.e., $p_2, p_3, \ldots$) will be very close to unity. Thus, a D will only rarely reach $n = 1$ from $n = 2$. Hence, our derivation of J_α in Eq. 2 will be perturbed very little by a small κ. Because of this, we can use J_α to make a very simple approximate calculation of the mean number $\bar{N}$ of GTP molecules (i.e., T subunits) in the GTP cap ($n = 2, 3, \ldots$) at the α end at steady state. With $\kappa > 0$, the cap will reach a steady size $\bar{N}$ at steady state. The rate of T entering the cap is J_α and the mean rate of T leaving the cap (becoming D) is $\kappa \bar{N}$. These quantities must be equal at steady state. Hence $\bar{N} = J_\alpha/\kappa$, where J_α is given by Eq. 2. Like J_α, $\bar{N}$ is linear in c. The smaller κ, the larger $\bar{N}$. This calculation is not accurate near $c = c_\alpha$, where $\bar{N}$ is relatively small.

If a subunit enters the cap (as a T) at time $t = 0$, the probability that it remains a T at a later time is $e^{-\kappa t}$ (as in radioactive decay). The relation between t and the position n reached by this subunit in the interior of the polymer is $t = (n - 2)/J_\alpha$. Hence,

$$p_n = \exp[-\kappa(n - 2)/J_\alpha]. \qquad [5]$$

There is an exponential decrease of p_n with n; the fall-off is slower with smaller κ.

THEORY: LOWER BRANCH, $J_\alpha < 0$

Here again we start with $\alpha_{1D} = 0$, $\kappa = 0$ and make a correction later for $\kappa > 0$. There is net steady shortening of the polymer in this case. The interior (n large) is all D and these Ds tend to be brought steadily to the surface ($n = 1$). However, because of the κ'' and α_{1T} transitions, it is still possible to build up a pure cap of Ts in positions $n = 2, 3, \ldots$. The cap is pure T, up to the boundary of interior Ds, because $\alpha_{1D} = 0$ and $\kappa = 0$. Fig. 3 shows the possible transitions and rate constants and also in-

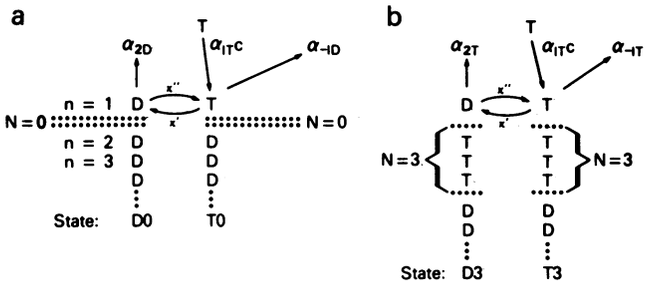

FIG. 3. Examples with $N = 0$ and $N = 3$ (number of T subunits in cap—i.e., at positions $n = 2, 3, \ldots$) of polymer states and possible transitions when $J_a < 0$ and $\kappa = 0$, $\alpha_{1D} = 0$.

troduces the possible states of the polymer end: DN and TN, with $N = 0, 1, 2, \ldots$. In this notation, D or T refers to the state of the end subunit ($n = 1$) whereas N specifies the number of Ts in the cap. Thus, in Fig. 3 *a* and *b*, we have $N = 0$ and $N = 3$, respectively. Note that the two off rate constants are different for $N = 0$ than they are for any $N > 0$.

Because all states of the polymer end can be classified as in Fig. 3 (both $\alpha_{1D} = 0$ and $\kappa = 0$ are necessary for this), it is possible to use the kinetic scheme interconnecting the states shown in Fig. 4. The constant α_{2D} does not appear in Fig. 4 because this transition in state D0 leaves the polymer in state D0. As we now show, the steady-state properties of the polymer are easy to deduce from Fig. 4.

The steady-state probabilities of the states in Fig. 4 are denoted p_{DN} and p_{TN}, with $N = 0, 1, \ldots$. The sum of all these is unity (normalization). The linear algebraic equations determining these probabilities are

$$dp_{D0}/dt = 0 = (\kappa' + \alpha_{-1D})p_{T0} - \kappa'' p_{D0}$$
$$dp_{T0}/dt = 0 = \kappa'' p_{D0} + \alpha_{2T} p_{D1} + \alpha_{-1T} p_{T1} - (\kappa' + \alpha_{-1D} + \alpha_{1T}c)p_{T0}, \quad [6]$$

etc., in the sequence D1, T1, D2, T2, etc. The D0 equation is special but the equations for the other states follow a repeating pattern. By working with the successive TN equations, using in each case the DN and D,$N + 1$ equations for eliminations, one finds the simple relations

$$p_{TN} = b p_{T,N-1} \qquad (N = 1, 2, \ldots) \quad [7]$$

and also (from the DN equations)

$$p_{T0} = a p_{D0}$$
$$p_{DN} = d p_{TN} \qquad (N = 1, 2, \ldots), \quad [8]$$

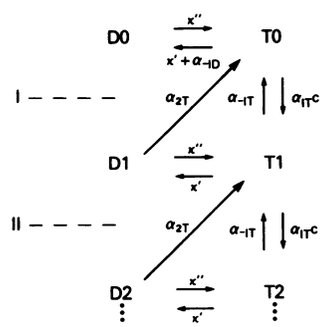

FIG. 4. Kinetic diagram for states of the polymer when $J_a < 0$ and $\kappa = 0$, $\alpha_{1D} = 0$.

where

$$a = \kappa''/(\kappa' + \alpha_{-1D}) \quad [9]$$

$$b = \frac{(\alpha_{2T} + \kappa'')\alpha_{1T}c}{\alpha_{2T}\kappa' + \alpha_{-1T}\alpha_{2T} + \alpha_{-1T}\kappa''} \quad [10]$$

$$d = \kappa'/(\alpha_{2T} + \kappa''). \quad [11]$$

If we now use Eqs. 7 and 8 to express all the other p_{DN} and p_{TN} in terms of p_{D0}, then the normalization relation leads to

$$p_{D0} = \frac{(1 - b)}{1 + a - b + abd} \quad [12]$$

and then

$$p_{TN} = \frac{ab^N(1 - b)}{1 + a - b + abd} \qquad (N = 0, 1, 2, \ldots) \quad [13]$$

$$p_{DN} = \frac{adb^N(1 - b)}{1 + a - b + abd} \qquad (N = 1, 2, \ldots). \quad [14]$$

The probability of a cap of size N is $p_{TN} + p_{DN}$.

Other quantities of interest are now easy to derive. The probability p_1 that position $n = 1$ is a T is (see Fig. 3)

$$p_1 = p_{T0} + p_{T1} + p_{T2} + \ldots = \frac{a}{1 + a - b + abd}. \quad [15]$$

Similarly, for higher n,

$$p_n = p_{T,n-1} + p_{Tn} + p_{T,n+1} + \ldots + p_{D,n-1} + p_{Dn} + p_{D,n+1} + \ldots = \frac{ab^{n-1}(1 + d)}{1 + a - b + abd} \qquad (n = 2, 3, \ldots). \quad [16]$$

The mean number of Ts in the cap ($n = 2, 3, \ldots$) is

$$\overline{N} = p_2 + p_3 + \ldots = \frac{ab(1 + d)}{(1 + a - b + abd)(1 - b)}. \quad [17a]$$

This can also be found from $p_{TN} + p_{DN}$ (above). We emphasize that this expression for $\overline{N}$ refers to a polymer with $\kappa = 0$ (no T $\rightarrow$ D in the polymer interior). If actually $\kappa > 0$, the above value of $\overline{N}$ is exaggerated. An approximate correction to $\overline{N}$ for $\kappa > 0$ is given in the next subsection.

From $p_{TN} + p_{DN}$ it is also easy to find the variance in N, which can be expressed in the form

$$\frac{\overline{N^2} - \overline{N}^2}{\overline{N}^2} = \frac{1 - b^2 + a + ab^2 d}{ab(1 + d)}. \quad [17b]$$

The probabilities p_{TT}, p_{TD}, p_{DT}, and p_{DD} are also of importance. The subscripts here refer to the states of the subunits in positions $n = 1, 2$. These four probabilities add to unity. From Fig. 3, we see that

$$p_{DD} = p_{D0}, \qquad p_{TD} = p_{T0} \quad [18]$$

$$p_{DT} = p_{D1} + p_{D2} + \ldots = \frac{abd}{1 + a - b + abd} \quad [19]$$

$$p_{TT} = p_{T1} + p_{T2} + \ldots = \frac{ab}{1 + a - b + abd}. \quad [20]$$

Note that

$$p_1 = p_{TD} + p_{TT}, \qquad p_2 = p_{DT} + p_{TT}. \quad [21]$$

Incidentally, in the uncorrelated approximation we would have

$p_{TT} = p_1 p_2$. It is easy to verify from Eqs. 15, 16, and 20 that this relationship does not hold here.

The net mean subunit flux J_α is given by

$$J_\alpha = \alpha_{1T} c p_1 - \alpha_{2D} p_{DD} - \alpha_{2T} p_{DT} - \alpha_{-1D} p_{TD} - \alpha_{-1T} p_{TT}. \quad [22]$$

The various terms are easy to understand from the subscripts. Actually, the p_1, p_{DT}, and p_{TT} terms in Eq. 22 cancel. This is because the total transition "traffic" across each of the lines I, II, . . . in Fig. 4 must be zero at steady state to provide a steady cap. The sum of this traffic over I, II, ... is expressed by the terms that cancel. Thus

$$\begin{aligned} J_\alpha(c) &= -\alpha_{2D} p_{DD} - \alpha_{-1D} p_{TD} \\ &= -\alpha_{2D} p_{D0} - \alpha_{-1D} p_{T0} \\ &= \frac{-(\alpha_{2D} + a\alpha_{-1D})(1 - b)}{1 + a - b + abd} \end{aligned} \quad [23]$$

Note that b is proportional to c (Eq. 10). At $c = 0$, $b = 0$, and the initial value of J_α (negative) is

$$J_\alpha(0) = \frac{-(\alpha_{2D} + a\alpha_{-1D})}{1 + a}. \quad [24]$$

At very small c (or b), J_α is linear in c (or b):

$$J_\alpha(c) = J_\alpha(0) - \frac{J_\alpha(0) ab(1 + d)}{1 + a} + \ldots. \quad [25]$$

Because $J_\alpha(0)$ is negative, the initial slope dJ_α/dc at $c = 0$ is always positive. Because a is proportional to κ'', the initial slope approaches zero if $\kappa'' \to 0$. One can show that both dJ_α/dc and d^2J_α/dc^2 are positive in $0 \leq c \leq c_\alpha$.

At the other limit in Eq. 23, $b \to 1$ and $J_\alpha(c) \to 0$. If we put $b = 1$ and $c = c_\alpha$ in Eq. 10, the resulting expression for c_α is the same as in Eq. 4. Thus, the two branches of J_α join at $J_\alpha = 0$, $c = c_\alpha$, though generally with a discontinuity in slope. Incidentally, we are now justified in writing $b = c/c_\alpha$. As $c \to c_\alpha$ (and $b \to 1$), all of the p_n ($n \geq 2$) $\to 1$ and $\bar{N} \to 1/(1 - b) \to \infty$ (see Eqs. 16 and 17). That is, the T cap becomes infinitely large (in the absence of interior hydrolysis, $\kappa = 0$). The variance in N also becomes infinitely large: the right-hand side of Eq. 17b approaches unity. The slope of the negative branch of $J_\alpha(c)$ near $c = c_\alpha$ is easily seen from Eq. 23 (using $b = c/c_\alpha$) to be

$$\left(\frac{dJ_\alpha}{dc}\right)_{c=c_\alpha} = \frac{\alpha_{2D} + a\alpha_{-1D}}{c_\alpha a(1 + d)}. \quad [26]$$

The slope of the positive branch of J_α is B in Eq. 3. Because $a \sim \kappa''$, at $c = c_\alpha$ the negative branch slope $\to \infty$ if $\kappa'' \to 0$. Recall that, at $c = 0$, the slope $\to 0$ if $\kappa'' \to 0$. Thus, as discussed above, there is a virtual phase transition at $c = c_\alpha$ if κ'' is small (with $\alpha_{1D} = 0$, $\kappa = 0$).

Using the relation $B = \alpha_{1T}/(1 + d)$, we find that the ratio of the two slopes at $c = c_\alpha$ is

$$\frac{\text{slope (negative branch)}}{\text{slope (positive branch)}} = \frac{\alpha_{2D} + a\alpha_{-1D}}{a\alpha_{1T} c_\alpha} = \frac{\kappa' \alpha_{2D} + \alpha_{-1D}\alpha_{2D} + \kappa''\alpha_{-1D}}{\kappa''\alpha_{1T} c_\alpha}. \quad [27]$$

This ratio $\to \infty$ as $\kappa'' \to 0$. We emphasize again that this result, Eq. 27, holds only for $\alpha_{1D} = 0$, $\kappa = 0$.

The rate of hydrolysis of GTP is simply $J_h = \kappa' p_1$, with p_1 given by Eq. 15.

Introduction of $\kappa > 0$. Before turning to the main topic of this subsection, we digress to consider $J_\alpha(c)$ at very small c (i.e., to the linear term in c) for arbitrary κ and α_{1D}. This is a generalization of Eq. 25, where $\kappa = 0$, $\alpha_{1D} = 0$. To obtain the linear term in $J_\alpha(c)$, it suffices to consider only the four states shown in Fig. 5 and transitions between them. These are the states in which T has not penetrated beyond $n = 1$ and $n = 2$. (Actually the same method can be extended numerically to provide the c^2, c^3, ... terms in J_α if we allow T to penetrate to $n = 3$, 4, ...) The normalized steady-state probabilities of the four states in Fig. 5 can be found as usual by solving the linear algebraic rate equations that follow from the figure. Then J_α is found from the on–off transitions in Fig. 5 plus the α_{2D} transition out of state DD (which does not change the state). Omitting details, the result is

$$J_\alpha(c) = J_\alpha(0) + \frac{C}{E^2 F}\alpha_{1T} c + \frac{G}{E^2}\alpha_{1D} c + \ldots, \quad [28]$$

where $J_\alpha(0)$ is the same as in Eq. 24 and

$$C = \kappa''(\kappa' + \kappa'' + \alpha_{2T})(\alpha_{2D}\kappa' + \alpha_{2D}\alpha_{-1D} + \alpha_{-1D}\kappa'' + \kappa E) + \kappa\kappa''[\alpha_{-1D}(\kappa' + \kappa'' + \alpha_{2D}) + \kappa E]$$

$$E = \kappa' + \kappa'' + \alpha_{-1D}$$

$$F = \alpha_{2T}\kappa' + \alpha_{2T}\alpha_{-1T} + \alpha_{-1T}\kappa'' + \kappa(\kappa' + \kappa'' + \alpha_{2T} + \alpha_{-1T} + \kappa)$$

$$G = (\kappa' + \alpha_{-1D})(\kappa' + \kappa'' + \alpha_{2D}).$$

This reduces to Eq. 25 if $\kappa = 0$, $\alpha_{1D} = 0$. Note that κ does not appear in the $\alpha_{1D}c$ term and that $C \to 0$ if $\kappa'' \to 0$, thus eliminating the $\alpha_{1T}c$ term. A significant initial slope in $J_\alpha(c)$ can occur only if there is an appreciable value of κ'' ($\alpha_{1T}c$ term) or of α_{1D} ($\alpha_{1D}c$ term) or both. These are the transitions that make it possible for T from solution to attach to the polymer end when c is very small.

The above result (Eq. 28) is exact. We turn now to an *approximate* correction of $\bar{N}$, the mean number of Ts in the cap, in Eq. 17a when κ is small but not zero ($\alpha_{1D} = 0$ still). When $\kappa \neq 0$, the derivation of Eqs. 12–23 is no longer valid: Figs. 3 and 4 no longer accommodate all possible states of the polymer because the cap is no longer pure T. However, when κ is small we take the following approximate approach. When $\kappa = 0$, a T that enters the cap (Fig. 3*b*) must eventually come back out of the cap—i.e., reach position $n = 1$ again—because the polymer is shortening. When $\kappa > 0$ but small, we assume that the average stochastic history of a T that enters and eventually leaves the cap is the *same* as when $\kappa = 0$ *except* for the fact that the T may "decay" to a D via the κ reaction during its lifetime in the cap. It is not difficult to correct $\bar{N}$ if we make this simpli-

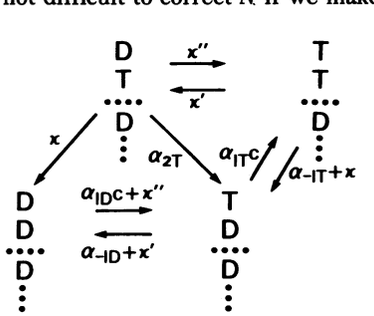

FIG. 5. Sufficient kinetic diagram to obtain exact properties of model near $c = 0$, including arbitrary κ and α_{1D}.

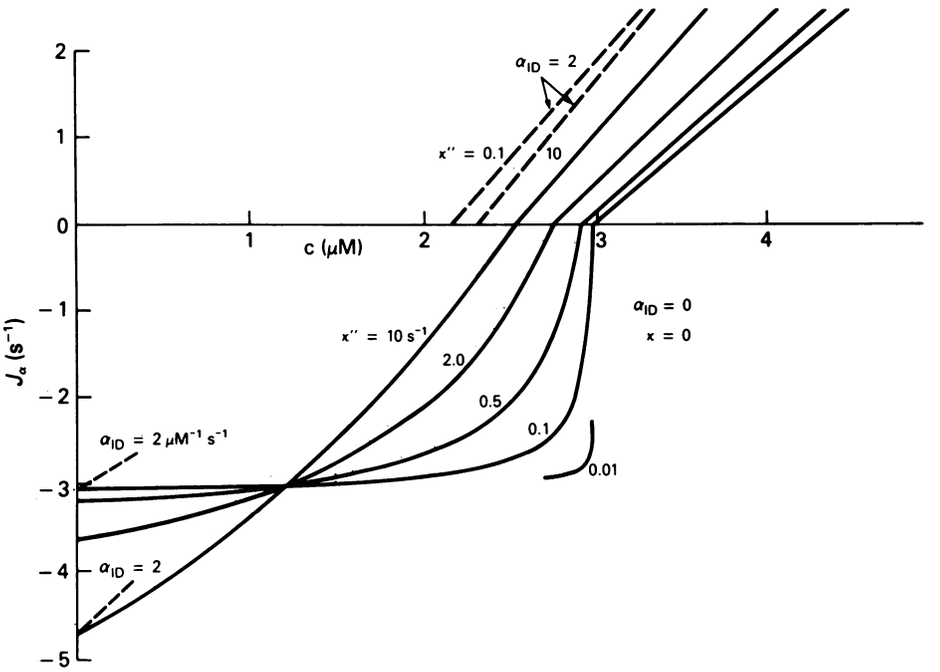

FIG. 6. J_α as a function of c for numerical example introduced in text. The solid curves are exact, for $\alpha_{1D} = 0$, $\kappa = 0$. The lower dashed lines show, in two cases, the effect of $\alpha_{1D} = 2$ near $c = 0$. These are also exact. The upper dashed lines, for the same two cases, are approximate (uncorrelated approximation).

fying assumption. The correction becomes very substantial indeed when $c \to c_\alpha$ because in this case the cap becomes very large ($\overline{N} \to \infty$ as $c \to c_\alpha$). As a consequence, a T entering the cap will generally change to D relatively early in its very long lifetime in the cap. Hence, when $c \to c_\alpha$ most of the uncorrected pure T cap will in fact have decayed to D, thus making the number of Ts in the corrected cap, $\overline{N}_{corr}$, much smaller than $\overline{N}$:‡

$$\overline{N}_{corr} \to (\alpha_{1T} c_\alpha / \kappa)^{1/2}. \quad [29]$$

NUMERICAL EXAMPLE

We illustrate the above theoretical results with a specific but rather arbitrary numerical example. All of the $J_\alpha(c)$ calculations in Fig. 6 are for the case $\kappa = 0$, though a small κ [e.g., 0.25 min^{-1}, as found experimentally (1)], would presumably hardly affect these curves except near $c = c_\alpha$ when κ'' is very small (10).

To begin with, we take $\alpha_{1D} = 0$. The other rate constants that we use are $\kappa' = 1.5\ s^{-1}$, $\alpha_{1T} = 2.5\ \mu M^{-1} s^{-1}$, $\alpha_{-1T} = \alpha_{-1D} = 6\ s^{-1}$, and $\alpha_{2T} = \alpha_{2D} = 3\ s^{-1}$. These rate constants are plausible values from data in the literature and relate to a single helix of the microtubule. The value of κ'' is varied. When $\kappa'' = 0$, $c_\alpha = 3\ \mu M$ (Eq. 4).

The lower branch ($J_\alpha < 0$) solid curves in Fig. 6 have been calculated from Eq. 23, for several values of κ'' (and $\alpha_{1D} = 0$ in all cases). Their intersection at $c = 1.2\ \mu M$ is an accidental degeneracy. For example, if we take $\alpha_{2D} \neq \alpha_{2T}$, the multiple intersection is broken up. The upper branch solid curves (straight lines) follow from Eq. 2. There is a discontinuity in slope at $c = c_\alpha$ ($J_\alpha = 0$), though this is small when $\kappa'' = 10\ s^{-1}$. Note how the initial slope of $J_\alpha(c)$ increases with κ''. When $\kappa'' \to 0$ (e.g., $\kappa'' = 0.01\ s^{-1}$), the transition from lower branch to upper branch becomes very sharp.

In the upper branch at, say, $J_\alpha = 1\ s^{-1}$ (any κ''), $\overline{N}$ (number of Ts in the cap) $\simeq J_\alpha/\kappa = 240$, if we take $\kappa = 0.25\ min^{-1}$. This is the number of Ts in one helix; there would be 1,200 in the microtubule if it is a five-start helix. To illustrate Eq. 29 for $\overline{N}_{corr}$ at $c = c_\alpha$, we use the $\kappa'' = 2\ s^{-1}$ case in Fig. 6. Then $c_\alpha = 2.76\ \mu M$ and $\overline{N}_{corr} \cong 41$.

The solid curves in Fig. 6 are for $\alpha_{1D} = 0$. The dashed lines illustrate the effect of $\alpha_{1D} > 0$. For these lines, we have taken $\alpha_{1D} = 2\ \mu M^{-1} \cdot s^{-1}$ and $\kappa'' = 0.1$ or $10\ s^{-1}$. The lower branch lines (near $c = 0$) are from Eq. 28 and are exact. Note that α_{1D} has a larger effect on the initial slope of $J_\alpha(c)$ when κ'' is small. The corresponding upper branch lines have been calculated using the uncorrelated approximation (4). They are probably quite accurate. Monte Carlo calculations would be needed to verify this and to fill in the missing parts of the dashed curves.

Related experiments will be reported on in a subsequent paper (11).

‡ Details of the derivation of Eq. 29 are available from T.L.H.

1. Carlier, M. F. & Pantaloni, D. (1981) *Biochemistry* **20**, 1918–1924.
2. Carlier, M. F. (1982) *Mol. Cell. Biochem.* **47**, 97–113.
3. Wegner, A. (1976) *J. Mol. Biol.* **108**, 139–150.
4. Hill, T. L. & Kirschner, M. W. (1982) *Int. Rev. Cytol.* **78**, 1–125.
5. Pardee, J. D. & Spudich, J. A. (1982) *J. Cell Biol.* **93**, 648–654.
6. Mockrin, S. C. & Korn, E. D. (1982) *J. Cell Biol.* **95**, 284a (abstr.).
7. Carlier, M. F. & Pantaloni, D. (1982) *Biochemistry* **21**, 1215–1224.
8. Weisenberg, R. C., Deery, W. J. & Dickinson, P. J. (1976) *Biochemistry* **15**, 4248–4254.
9. David-Pfeuty, T., Erickson, H. P. & Pantaloni, D. (1977) *Proc. Natl. Acad. Sci. USA* **74**, 5372–5376.
10. Chen, Y. & Hill, T. L. (1983) *Proc. Natl. Acad. Sci. USA*, in press.
11. Carlier, M. F., Hill, T. L. & Chen, Y. (1984) *Proc. Natl. Acad. Sci. USA*, in press.